Synthesis of Multi-Beam Space-Tapered Linear Arrays with Side Lobe Level Minimization in the Presence of Mutual Coupling

Aslan, Yanki; Candotti, Massimo; Yarovoy, Alexander

Synthesis of Multi-Beam Space-Tapered Linear Arrays with Side Lobe Level Minimization in the Presence of Mutual Coupling

Yanki Aslan[1], Massimo Candotti[2], Alexander Yarovoy[1]

[1] MS3 Group, Department of Microelectronics, Faculty of EEMCS, TU Delft, The Netherlands
Y.Aslan@tudelft.nl, A.Yarovoy@tudelft.nl
[2] Independent consultant, London, UK
massimo.candotti@gmail.com

***Abstract*—An iterative convex element position optimization algorithm is proposed for linear phased array synthesis with the aim of minimizing the side lobe level at multiple scan angles in the presence of mutual coupling. Embedded element patterns are obtained via full-wave simulations and integrated into the optimization procedure. A two-step optimization scheme with a smart initial array layout selection is proposed and analyzed. Conventional H-plane patch antenna arrays are used for algorithm demonstration. The simulation results show that via position-only optimization, the maximum side lobe level can be significantly decreased compared to the benchmark regular arrays with a half-wavelength spacing while keeping a similar total array length.**

***Index Terms*—antenna array synthesis, aperiodic array, convex optimization, fifth generation (5G) communication, multi-beam array, mutual coupling, space tapering.**

I. Introduction

The growing demand for meeting the challenging 5G system requirements on the channel capacity gains, front-end circuitry design aspects, cost and signal processing complexity favors exploiting unconventional array topologies rather than commonly used regular layouts that are based on square or triangular lattices [1]–[3]. Thinned arrays [4]–[6] and sparse arrays [7]–[9] are two techniques that are included in the unconventional array architectures and show good potential for 5G systems since they can address the multidisciplinary challenges.

An interesting combination of thinning and sparsity results in the concept of space tapering for which the amplitude of each element is fixed and the positions can be determined or changed freely. This is particularly attractive in 5G applications at mm-waves since space tapered arrays are able to provide the optimum power efficiency while suppressing the side lobe levels to some extent. Similar to the thinned and sparse arrays, a large variety of uniform amplitude irregular array synthesis methods exist in the literature. Many global optimization algorithms [10], [11] and deterministic synthesis techniques [12], [13] have been effectively used to design space tapered arrays with sufficiently low side lobes.

Recently, iterative convex optimization techniques have been extensively used in antenna synthesis [14]–[20] due to their superiority in terms of reduced computational and analytical complexity as compared to the existing methods. However, in most of these studies, and also in the other synthesis techniques given until this point, antenna elements have been taken either as isotropic sources or identical patterns have been assumed for every antenna element. In other words, the effect of mutual coupling has been ignored. Although design-based mutual coupling methods [21]–[23] can be exploited to reduce the mutual coupling, these techniques do not completely remove the mutual coupling effect and introduce additional design complexity. There are some studies focusing on compensating the effect of mutual coupling in the synthesis process [24], which is very challenging to achieve by position-only optimization. Other studies have included the mutual coupling effect in the array synthesis using several techniques, such as infinite-to-finite array approach [25], neural networks [26] and spherical wave expansion [27]. Recently, a more comprehensive gradient-based technique has been proposed in [28], which can be used for the synthesis of aperiodic arrays with various types of radiators (dipoles, apertures, dielectric resonators etc.).

In iterative convex optimization for aperiodic array synthesis, inclusion of mutual coupling in the design procedure was first introduced in [17] which proposed a two-step design approach for the synthesis of sparse arrays of dipoles. In the first step, the optimization was performed by assuming the same isolated element pattern (IEP) for each dipole. Using the result as an initial guess, in the second step, embedded element pattern (EEP) of each element was obtained via full-wave simulations and used in the same optimization routine. It was shown that convergence in the minimized max. SLL can be achieved after only a few iterations. Later, in [18], the optimization technique applied only to the broadside beam in [17] was extended to multiple scan angles. The disadvantage

of these techniques in [17], [18] was the applied amplitude tapering with a large dynamic range. Motivated by this, in [29], the space-tapering method in [16] was improved by including the mutual coupling effect using a single-step fast full-wave simulation technique (i.e. optimization with embedded patterns, without an initial guess) and the performance was demonstrated using practical bowtie antenna elements. Extension of [29] to larger linear and planar arrays was presented in [30]. Although being able to address the issue with amplitude tapering, the methods in [29], [30] did not provide optimization for multiple beams at different scan angles and they were not suitable for 5G cellular communication.

A method for position-only tapering with multi-beam optimization for minimizing the maximum SLL was introduced in [19], [20] for 5G base station applications. However, identical element patterns were assumed and mutual coupling was ignored during the optimization. In this paper, the technique in [19] is extended by including the mutual coupling in the design procedure. The proposed novel method combines the advantages of the previously proposed array synthesis techniques in the presence of mutual coupling, namely, multi-beam optimization from [18] and uniform excitation from [29].

The remainder of the paper is organized as follows. In Section II, formulation of the optimization problem and optimization procedure used in this work are presented. Section III provides numerical examples using linear patch antenna arrays. Discussions on the results are also given. Section IV concludes the paper.

II. Methodology

A. Problem Formulation

Let us consider an N-element linear array with the geometry given in Fig. 1.

The far field radiated by this array is given by

$$f(\theta,\phi)=\sum_{n=1}^{N} f_n(\theta,\phi)w_n e^{jk_0\sin\theta\cos\phi x_n} \tag{1}$$

where $f_n(\theta,\phi)$ is the complex far-field of the n^{th} element when the field origin is at the element's own geometrical center, k is the wavenumber, x_n and w_n are the position and excitation weight of the n^{th} element, respectively.

At the θ=90 degree cut, (1) can be expressed as

$$f(\theta=90,\phi)=\sum_{n=1}^{N} f_n(\theta=90,\phi)w_n e^{jk_0\cos\phi x_n} \tag{2}$$

Now, assume the array is uniformly-excited and the beam is scanned at p different angles. ϕ_{s_m} represents the direction of maximum radiation for the scanned beam $s_{m=1,2,\ldots,p}$. In this case, the weight of the n^{th} element for the scan angle ϕ_{s_m} is given by

$$w_{n,s_m}=e^{-jk_0\cos\phi_{s_m}x_n} \tag{3}$$

Thus, the far-field of a uniformly-excited array at the θ=90 degree cut for the scan angle ϕ_{s_m} becomes

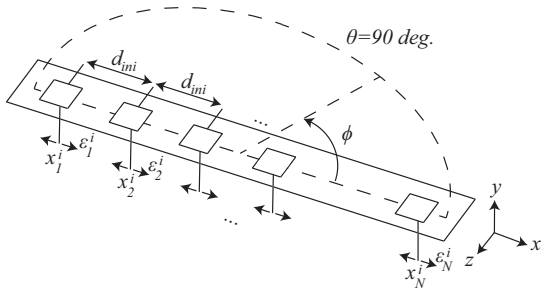

Fig. 1. Geometry of a linear array of N patch antennas.

$$f(\theta=90,\phi)=\sum_{n=1}^{N} f_n(\theta=90,\phi)e^{jk_0(\cos\phi-\cos\phi_{s_m})x_n} \tag{4}$$

Using the first-order Taylor expansion $e^{j\Phi}=1+j\Phi$, where $\Phi=k_0(\cos\phi-\cos\phi_{s_m})\epsilon_n^i$, in (4) around x_n, the far-field of the array at the i^{th} iteration for the scanned beam s_m at the θ=90 degree cut can be linearly approximated by

$$f_{\epsilon_n}^{i,s_m}(\theta=90,\phi)\approx\sum_{n=1}^{N} f_n^i(\theta=90,\phi)e^{jk_0(\cos\phi-\cos\phi_{s_m})x_n^{i-1}} (1+jk_0(\cos\phi-\cos\phi_{s_m})\epsilon_n^i) \tag{5}$$

where x_n^{i-1} is the position of the n^{th} element at the previous iteration and ϵ_n^i is the position shift of the n^{th} element at the i^{th} iteration, as visualized in Fig. 1. Note that initially the elements are regularly placed with a separation of d_{ini}.

Let us define the side lobe region for each scan angle according to a pre-specified beam width, ϕ_b such that

$$\phi\in\boldsymbol{\phi_{SL,s_m}}\ if\ \phi<(\phi_{s_m}-\phi_b)\ or\ \phi>(\phi_{s_m}+\phi_b) \tag{6}$$

Following the formulation in [19], the convex problem to be solved at the i^{th} iteration of the algorithm can be formulated as follows

$$\min_{\boldsymbol{\epsilon}^i}\rho,\quad s.t.\ \begin{cases}|f_{\boldsymbol{\epsilon}^i}^{i,s_m}(\theta=90,\boldsymbol{\phi_{SL,s_m}})|\le\rho\ \text{for}\ \forall s_m\\ |\boldsymbol{\epsilon}^i|\le\mu\\ D^*(\boldsymbol{\epsilon}^i+\boldsymbol{x}^{i-1})\ge d_{\min}\end{cases} \tag{7}$$

where ρ is the maximum side lobe level which is simultaneously minimized for all the defined scan angles in a sector, μ is a user-defined upper-bound for the position shifts and D is an $(N-1)\times N$ circulant matrix (see [19]) that is used for guaranteeing a desired minimum inter-element spacing ($d_{\min}$) at each iteration of the algorithm. If needed, it is also possible to enforce symmetry in the final layout by adding another constraint on $\boldsymbol{\epsilon}^i$ such that ϵ_n^i = - ϵ_{N-n+1}^i. The problem in (7) is a second-order cone program that can be efficiently solved using interior point methods.

B. Optimization Procedure

The candidate iterative optimization schemes, namely the one-step [29] and two-step (a modified version of [17]) approaches, are summarized in Fig. 2 and Fig. 3, respectively. In the single-step approach, starting from an initial regular

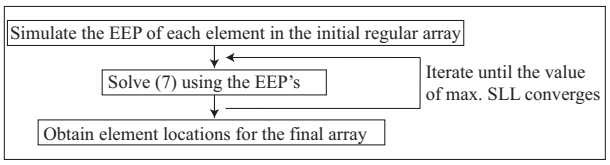

Fig. 2. One-step optimization scheme.

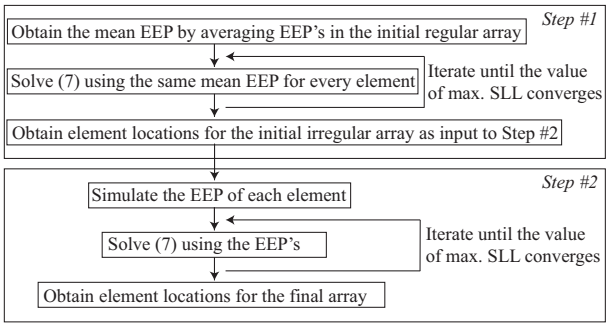

Fig. 3. Two-step optimization scheme.

array with spacing d_{ini}, the array is simulated in sequential mode to obtain EEP's of all elements at each iteration. In the two-step approach, on the other hand, the average EEP (obtained from the initial regular array with spacing d_{ini}) is used to optimize the element locations with no mutual coupling (similarly as previously done in [19], but now the mean EEP carries the average amplitude and phase information due to mutual coupling within the array elements in Step #1). Using these locations as an initial guess, embedded far-field of each element is simulated at each iteration in Step #2 and integrated into the optimization routine to obtain the final array layout. In this paper, the two-step approach is used because of its proven efficiency in optimization time [17].

III. Numerical Results

All simulations in this section have been carried out on an Intel(R) Core(TM) i7-6700HQ 2.6GHz CPU, 16 GB RAM computer using EMPIRE XPU, CVX and MATLAB®.

The algorithm has been tested for an example case using a 16-element H-plane linear patch antenna array fed by lumped ports [33] and optimized in a ± 30 degree scan angle range with 10 degree steps. It is worth to mention here that the algorithm can be straightforwardly applied to E-plane arrays, arrays of different radiators or an array of more complex 5G sub-array designs, such as [31], at the expense of increased simulation time and modeling complexity.

The observation angle, ϕ, has been discretized in 0.5 degree steps and the beam width, ϕ_b has been taken as 8 degrees. Visualization of a sample irregular H-plane array and its important design parameters are provided in Fig. 4 and Table I, respectively.

The convergence analyses have been performed by observing the max. SLL at each iteration of the algorithm. The inter-element spacing, d_{ini}, and the minimum allowed inter-element spacing, $d_{\min}$, have been selected as $0.35\lambda_0$ in Step #1 of the two-step optimization scheme.

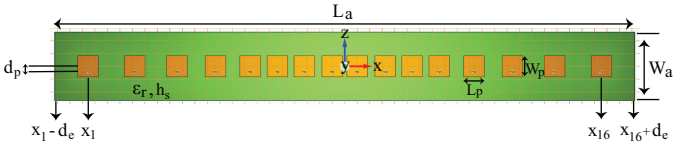

Fig. 4. A sample space-tapered 16-element H-plane array in EMPIRE XPU with its important dimensions.

TABLE I
List of design parameters used in EMPIRE XPU

Parameter definition	Symbol	Value
Center frequency*	f_0	28 GHz
Relative permittivity of the substrate	ϵ_r	2.2
Patch substrate thickness	h_s	0.5 mm
Patch width	W_p	3.3 mm
Patch length	L_p	3.3 mm
Array width	W_a	λ_0
Array edge offset	d_e	$0.5\lambda_0$
Array length	L_a	$x_{16} - x_1 + \lambda_0$
Patch feeding offset	d_p	0.9 mm

* The center frequency has been selected considering a candidate 5G frequency band that has a growing interest [32].

First, a 16-element regular H-plane array with $d_{ini} = 0.35\lambda_0$ has been sequentially simulated for different mesh resolutions in EMPIRE. Table II shows the mesh information and simulation times to obtain 16 EEP's. Among the listed meshing options, medium resolution has been selected to be used in the rest of the paper since it has been seen to provide a good compromise between simulation time and accuracy. For the medium resolution mesh, the embedded field amplitudes and phases for the dominant E-field component, E_θ, are given in Fig. 5, which clearly shows the effect of mutual coupling. At this point it is worthy of note that the relatively large back lobe (approximately -18 dB) is due to the limited ground plane dimensions, which can be further improved. Here, we will focus on the SLL minimization in the forward radiation hemisphere.

The effect of varying the upper-bound of position shifts, μ, in Step #1 of the two-step optimization scheme has also been studied and the result is given in Fig. 6. In Step #1, the use of the average EEP within the optimization process produces a smooth converge path to a well-defined max. SLL, similarly to what was observed in [19].

Next, the two-step procedure has been completed by performing Step #2 in Fig. 3 using the layout obtained in the analysis given in Fig. 6 with $\mu = 0.02\lambda_0$ (due to its smallest

TABLE II
List of mesh parameters used in EMPIRE XPU **

Resolution	CW	CO	SP	NR	t_{avg} (mins)
Coarse	10	3	5000	1	13
Medium	15	4	10000	5	19
Fine	20	5	20000	10	29
Very fine	25	6	40000	15	59

** CW = Cells/Wavelength, CO = Cells/Object, SP = Search Points, NR = Numeric Resolution. The values are taken from [33]. t_{avg} is the average time required for sequential excitation of array elements to obtain 16 embedded field patterns.

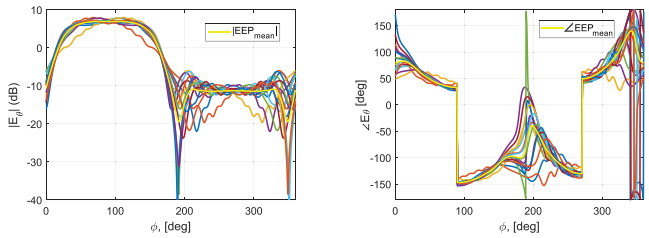

(a) (b)

Fig. 5. Embedded electric field amplitudes and phases of 16 elements in a regular H-plane array with $d_{ini} = 0.35\lambda_0$.

SLL among all) as the initial guess. The convergence trend in Step #2 of the two-step optimization scheme is indicated in Fig. 7. Conversely to Step #1, in Step #2, the max. SLL convergence for different μ show relatively irregular paths. The ripple in the final value, as iterations are carried out, tends to be larger with increased μ, as seen in Fig. 7. This can be related to the convex optimization process in that for relatively larger values in the optimized function domain, the results tend to 'escape' the global minimum, for later on reaching it again and so on. Thus, for a more stable convergence in Step #2, μ should be chosen as $0.02\lambda_0$, which also guarantees a lower max. SLL. Nevertheless, it is worth to note that the ripple in the convergence for larger μ are limited to only ± 0.3 dB for $\mu = 0.08\lambda_0$. This aspect of the converge can be used as trade-off between reaching a certain max. SLL versus the number of iterations allowed or budgeted for the whole optimization.

From Fig. 6 and Fig. 7, it has been seen that the max. SLL obtained in Step #1 is actually larger by about 2.4 dB (-19.8 dB in Fig. 6 and -17.4 dB at the first step in Fig. 7) due to the mutual coupling. However, convergence to -18.5 to -19 dB

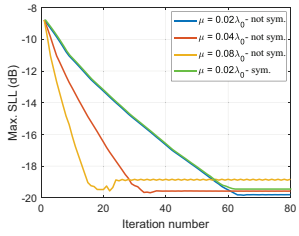

Fig. 6. Effect of varying μ on the convergence performance in Step #1 of the two-step optimization with $d_{\min} = 0.35\lambda_0$.

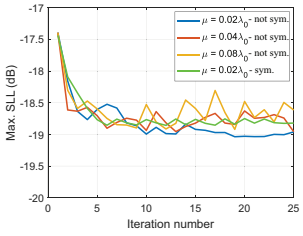

Fig. 7. Convergence in Step #2 of the two-step optimization scheme with $d_{\min} = 0.35\lambda_0$ and varying μ.

TABLE III
SUMMARY OF MAX. SLL AND SIMULATION TIME COMPARISON FOR THE TWO-STEP OPTIMIZATION SCHEME WITH $\mu = 0.02\lambda_0$ FOR DIFFERENT MAXIMUM TOLERABLE SLL OF A SYSTEM

Layout symmetry	Max. tolerable SLL (dB)	Min. required iteration number	Observed max. SLL (dB)	Increase in array length (%) ***	Optimization time (mins)
No	-18	2	-18.16	3.73	55.85
	-18.5	3	-18.64	4.27	85.53
	-19	10	-19.00	5.07	300.98
Yes	-18	2	-18.09	2.40	44.52
	-18.5	4	-18.59	3.47	88.70
	-19	NA	NA	NA	NA

NA = Not Available. *** Increase in array length shows the array length variation in % against the benchmark $0.5\lambda_0$ equispaced array which has a total length of $7.5\lambda_0$.

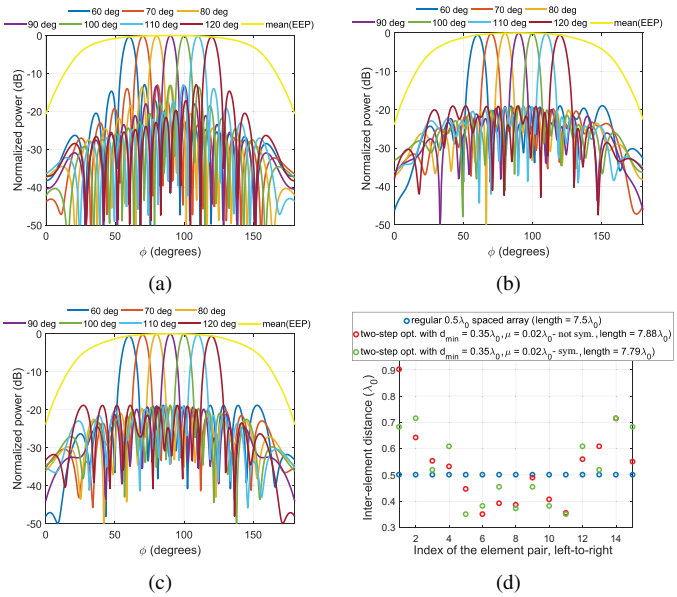

(a) (b) (c) (d)

Fig. 8. Performance comparison of the $0.5\lambda_0$-spaced regular array and output of the two-step optimization with $\mu = 0.02\lambda_0$ at iteration number 25, (a) far-field pattern - regular array, (b) far-field pattern - two-step opt. - not symmetrical layout, (c) far-field pattern - two-step opt. - symmetrical layout, (d) inter-element spacings.

band has been obtained only in 2 additional iterations for all the investigated cases in Fig. 7. A final 'stable' convergence to -19 dB and -18.8 dB has been observed for $\mu = 0.02\lambda_0$ in the non-symmetrical and symmetrical cases, respectively.

The radiation patterns and inter-spacings in the regular and optimized arrays for $\mu = 0.02\lambda_0$ are shown in Fig. 8. A comparison of the max. SLL, array length and simulation time for the two-step optimization scheme with $\mu = 0.02\lambda_0$ for different maximum tolerable SLL's is given in Table III.

IV. CONCLUSION

A uniform amplitude, space tapered, linear phased array synthesis technique has been proposed by taking into account the effect of mutual coupling between the array elements.

The technique in [19] has been extended by including the embedded element patterns into the optimization procedure via full-wave simulations. The advantages of the previously proposed mutual coupling aware array synthesis techniques have been combined in a single optimization algorithm by including the multi-beam optimization from [18] and uniform excitation from [29].

The proposed method's performance has been demonstrated using a 16-element H-plane linear patch antenna array at 28 GHz with SLL minimization in a ± 30 degree scan range. A two-step optimization scheme (with an optimized initial layout using the mean EEP of the regular array as an isolated element pattern) has been exploited due to its efficiency in optimization time. The choice of relatively closely-packed elements in the initial array configuration with $0.35\lambda_0$ equispaced separation, rather than the $0.5\lambda_0$ element separation from standard antenna array design practice, allowed increased mutual coupling within elements leading to a final optimized max. SLL as

low as -19 dB compared to the -13 dB of a same number of elements $0.5\lambda_0$ equispaced array, while keeping a similar total array length (only 4-5% increase).

It is worthy of note that the end result of the optimization depends heavily on the selection of input parameters (such as ϕ_b, μ, d_{ini}, $d_{\min}$, and so on) and the initial array topology. All these aspects can be easily investigated by the interested readers using different sets of initial parameter values.

Care must be taken when calculating the far-field with active elements while using EMPIRE. In EMPIRE, the total surrounding near field is used for far field calculation which is of course limited by the boundaries. By default the boundaries are chosen to be λ/4 apart to the antenna which may be to small for large arrays. Thus, it is good practice to perform convergence tests on the total far-field obtained with active elements excitation versus size of the simulation box.

The proposed algorithm can be straightforwardly applied to the arrays of different types of radiators (dipoles, horns, dielectric resonators, cavity-backed antennas etc.) or phased arrays of more complex sub-arrays, such as [31], which are suitable for 5G base stations.

ACKNOWLEDGMENT

This research was conducted as part of the NWO-NXP Partnership Program on Advanced 5G Solutions within the project titled "Antenna Topologies and Front-end Configurations for Multiple Beam Generation". More information: www.nwo.nl.

The authors would like to thank IMST GmbH (Germany) for granting the use of the EMPIRE XPU Finite Difference Time Domain (FDTD) simulation software and for their technical support.

REFERENCES

[1] P. Rocca, G. Oliveri, R. J. Mailloux and A. Massa, "Unconventional phased array architectures and design methodologies - A review," *Proc. IEEE*, vol. 104, no. 3, pp. 544–560, Jan. 2016.

[2] Y. Aslan, J. Puskely, J. H. J. Janssen, M. Geurts, A. Roederer and A. Yarovoy, "Thermal-aware synthesis of 5G base station antenna arrays: an overview and a sparsity-based approach," *IEEE Access*, vol. 6, pp. 58868–58882, Oct. 2018.

[3] X. Ge, R. Zi, H. Wang, J. Zhang and M. Jo, "Multi-user massive MIMO communication systems based on irregular antenna arrays," *IEEE Trans. Wireless Commun.*, vol. 15, no. 8, pp. 5287-5301, Aug. 2016.

[4] B. V. Ha, M. Mussetta, P. Pirinoli and R. E. Zich, "Modified compact-genetic algorithm for thinned array synthesis," *IEEE AWPL*, vol. 15, pp. 1105-1108, Oct. 2015.

[5] O. Q. Teruel and E. R. Iglesias, "Ant colony optimization inthinned array synthesis with minimum sidelobe level," *IEEE AWPL*, vol. 5, pp. 349-352, Dec. 2006.

[6] G. Oliveri, L. Manica and A. Massa, "ADS-based guidelines for thinned planar arrays," *IEEE Trans. Antennas Propag.*, vol. 58, no. 6, pp. 1935-1948, Jun. 2010.

[7] Y. Liu, Q. H. Liu and Z. Nie, "Reducing the number of elements in multiple-pattern linear arrays by the extended matrix pencil methods," *IEEE Trans. Antennas Propag.*, vol. 62, no. 2, pp. 652-660, Nov. 2013.

[8] F. Yan, P. Yang, F. Yang and T. Dong, "Synthesis of planar sparse arrays by perturbed compressive sampling framework," *IET Microw. Antennas Propag.*, vol. 10, no. 11, pp. 1146–1153, Aug. 2016.

[9] A. Massa, P. Rocca and G. Oliveri, "Compressive sensing in electromagnetics - A review," *IEEE Antennas Propag. Mag*, vol. 57, no. 1, pp. 224-238, Feb. 2015.

[10] D. G. Kurup, M. Himdi and A. Rydberg, "Synthesis of uniform amplitude unequally spaced antenna arrays using the differential evolution algorithm," *IEEE Trans. Antennas Propag.*, vol. 51, no. 9, pp. 2210–2217, Sep. 2003.

[11] K. Chen, Z. He and C. Han, "A modified real GA for the sparse linear array synthesis with multiple constraints," *IEEE Trans. Antennas Propag.*, vol. 54, no. 7, pp. 2169–2173, Jul. 2006.

[12] O. M. Bucci, M. D'Urso, T. Isernia, P. Angeletti and G. Toso, "Deterministic synthesis of uniform amplitude sparse arrays via new density taper techniques," *IEEE Trans. Antennas Propag.*, vol. 58, no. 6, pp. 1949–1958, Jun. 2010.

[13] A. F. Morabito, T. Isernia and L. Di Donato, "Optimal synthesis of phase-only reconfigurable linear sparse arrays having uniform-amplitude excitations," *Prog. Electromagn. Res.*, vol. 124, pp. 405–423, 2012.

[14] P. You, Y. Liu, S. L. Chen, K. D. Xu, W. Li and Q. H. Liu, "Synthesis of unequally spaced linear antenna arrays with minimum element spacing constraint by alternating convex optimization," *IEEE APWL*, vol. 16, pp. 3126–3130, Oct. 2017.

[15] G. Prisco and M. D'Urso, "Maximally sparse arrays via sequential convex optimization," *IEEE Antennas Wireless Propag. Lett.*, vol. 11, pp. 192–195, Feb. 2012.

[16] B. Fuchs, A. Skrivervik and J R. Mosig, "Synthesis of uniform amplitude focused beam arrays," *IEEE Antennas Wireless Propag. Lett.*, vol. 11, pp. 1178–1181, Oct. 2012.

[17] C. Bencivenni, M. V. Ivashina, R. Maaskant and J. Wettergren, "Design of maximally sparse antenna arrays in the presence of mutual coupling," *IEEE Antennas Wireless Propag. Lett.*, vol. 14, pp. 159–162, Sep. 2014.

[18] C. Bencivenni, M. V. Ivashina, R. Maaskant and J. Wettergren, "Synthesis of maximally sparse arrays using compressive sensing and full-wave analysis for global earth coverage applications," *IEEE Trans. Antennas Propag.*, vol. 64, no. 11, pp. 4872–4877, Jul. 2016.

[19] Y. Aslan, J. Puskely, A. Roederer and A. Yarovoy, "Synthesis of multiple beam linear arrays with uniform amplitudes," in *Proc. 12th EuCAP*, London, UK, Apr. 2018.

[20] Y. Aslan, J. Puskely, A. Roederer and A. Yarovoy, "Multiple beam synthesis of passively cooled 5G planar arrays using convex optimization," *IEEE Trans. Antennas Propag.*, submitted for publication.

[21] Y. Aslan and A. Yarovoy, "Reduction of mutual coupling between closely spaced patch antennas using dielectric stratification technique," in *Proc. 47th EuMC*, Nuremberg, Germany, pp. 248–251, Oct. 2017.

[22] E. R. Iglesias, O. Q. Teruel and L. I. Sanchez, "Mutual coupling reduction in patch antenna arrays by using a planar EBG structure and a multilayer dielectric substrate," *IEEE Trans. Antennas Propag.*, vol. 56, no. 6, pp. 1648–1655, Jun. 2008.

[23] C. Y. Chiu, C. H. Cheng, R. D. Murch and C. R. Rowell, "Reduction of mutual coupling between closely-packed antenna elements," *IEEE Trans. Antennas Propag.*, vol. 55, no. 6, pp. 1732–1738, Jun. 2007.

[24] T. Zhang and W. Ser, "Robust beampattern synthesis for antenna arrays with mutual coupling effect," *IEEE Trans. Antennas Propag.*, vol. 59, no. 8, pp. 2889–2895, Aug. 2011.

[25] J. I. Echeveste, M. A. Gonzalez de Aza and J. Zapata, "Array pattern synthesis of real antennas using the infinite-array approach and linear programming," *IEEE Trans. Antennas Propag.*, vol. 63, no. 12, pp. 5417–5424, Dec. 2015.

[26] R. G. Ayestaran, F. L. Heras and L. F. Herran, "Neural modeling of mutual coupling for antenna array synthesis," *IEEE Trans. Antennas Propag.*, vol. 55, no. 3, pp. 832–840, Mar. 2007.

[27] J. Corcoles, J. Rubio and M. A. Gonzalez, "Spherical-wave-based shaped-beam field synthesis for planar arrays including the mutual coupling effects," *IEEE Trans. Antennas Propag.*, vol. 59, no. 8, pp. 2872–2881, Aug. 2011.

[28] J. I. Echeveste, M. A. Gonzalez de Aza, J. Rubio and C. Craeye, "Gradient-based aperiodic array synthesis of real arrays with uniform amplitude excitation including mutual coupling," *IEEE Trans. Antennas Propag.*, vol. 65, no. 2, pp. 541–551, Feb. 2017.

[29] H. B. Van, S. N. Jha and C. Craeye, "Efficient array synthesis of printed arrays including mutual coupling," in *Proc. 10th EuCAP*, Davos, Switzerland, Apr. 2016.

[30] H. B. Van, S. N. Jha and C. Craeye, "Fast full-wave synthesis of printed antenna arrays including mutual coupling," *IEEE Trans. Antennas Propag.*, vol. 64, no. 12, pp. 5163–5171, Dec. 2016.

[31] J. Puskely, Y. Aslan, A. Roederer and A. Yarovoy, "SIW based antenna array with power equalization in elevation plane for 5G base stations," in *Proc. 12th EuCAP*, London, UK, Apr. 2018.

[32] GSM Association, "5G spectrum – 26 GHz and 28 GHz," *GSMA Spectrum*, Sept. 2018.

[33] IMST GmbH, "EMPIRE XPU version 7.50," *Software Manual*, Aug. 2016.